HHS Public Access

Author manuscript

Neurobiol Aging. Author manuscript; available in PMC 2022 February 01.

Published in final edited form as:

Neurobiol Aging. 2021 February ; 98: 231–241. doi:10.1016/j.neurobiolaging.2020.11.012.

Cross-sectional and longitudinal Medial Temporal Lobe Subregional Atrophy Patterns in Semantic Variant Primary Progressive Aphasia

L.E.M. Wisse[1,2,3,a], **M.B. Ungrady**[4], **R. Ittyerah**[1], **S.A. Lim**[1], **P.A. Yushkevich**[1], **D.A. Wolk**[2], **D. J. Irwin**[4,5], **S.R. Das**[2,*], **M. Grossman**[4,*]

[1]Department of Radiology, University of Pennsylvania, Philadelphia, PA 19104, USA

[2]Department of Neurology, Penn Memory Center, University of Pennsylvania, Philadelphia, PA 19104, USA

[3]Department of Diagnostic Radiology, Lund University, Lund, 22242, Sweden

[4]Department of Neurology, Penn Frontotemporal Degeneration Center, University of Pennsylvania, Philadelphia, PA 19104, USA

[5]Department of Pathology and Laboratory Medicine, University of Pennsylvania School of Medicine Center for Neurodegenerative Disease Research (CNDR), University of Pennsylvania, Philadelphia, PA 19104, USA

Abstract

Introduction: T1-MRI studies report early atrophy in the left anterior temporal lobe, especially the perirhinal cortex (PRC), in semantic variant Primary Progressive Aphasia (svPPA). Improved segmentation protocols using high-resolution T2-MRI have enabled fine-grained medial temporal lobe (MTL) *subregional* measurements, which may provide novel information on the atrophy pattern and disease progression in svPPA. We aimed to investigate the MTL subregional atrophy pattern cross-sectionally and longitudinally in patients with svPPA as compared to controls and patients with Alzheimer's disease (AD).

Methods: MTL subregional volumes were obtained using the Automated Segmentation for Hippocampal Subfields (ASHS) software from high-resolution T2-MRIs in 15 svPPA, 37 AD and 23 healthy controls. All MTL volumes were corrected for intracranial volume and parahippocampal cortices for slice number. Longitudinal atrophy rates of all subregions were obtained using an unbiased deformation-based morphometry pipeline in 6 svPPA patients, 9 controls and 12 AD patients.

Corresponding author: Laura E.M. Wisse, Diagnostic Radiology, Lund University, Remissgatan 4, 222 42 Lund, Sweden, lemwisse@gmail.com.

[a]Performed the statistical analyses

[*]Shared last author

Conflicts of interest.

None of the authors has any disclosures, except Dr. Wolk who reports grants from Avid/Lilly, grants from Merck, grants from Biogen, grants from Functional Neuromodulation, personal fees from Neuronix, outside the submitted work, and Dr. Grossman who reports grants from Biogen, PassageBio, Bracco, Avid/Lilly, Life Molecular Imaging, and participation in treatment trials sponsored by Biogen, Eisai and UCB unrelated to this work.

Results: Cross-sectionally, significant volume loss was observed in svPPA compared to controls in the left MTL, right cornu ammonis (CA)1, Brodmann Area (BA)35 and BA36 (subdivisions of the PRC). Compared to AD patients, svPPA patients had significantly smaller left CA1, BA35 and left and right BA36 volumes. Longitudinally, svPPA patients had significantly greater atrophy rates of left and right BA36 compared to controls, but not relative to AD patients.

Discussion: Fine-grained analysis of MTL atrophy patterns provides information about the evolution of atrophy in svPPA. These results indicate that MTL subregional measures might be useful markers to track disease progression or for clinical trials in svPPA.

Keywords

semantic variant primary progressive aphasia; longitudinal; medial temporal lobe; atrophy; perirhinal cortex

Introduction

Semantic variant progressive primary aphasia (svPPA), also referred to as semantic dementia, is a variant of frontotemporal dementia (Gorno-Tempini et al., 2011, Hodges, John R. and Patterson, 2007) that is characterized by progressive impairments in conceptual knowledge, naming and word finding difficulties. Moreover, svPPA is characterized by volume loss particularly in the left anterior temporal lobe (Davies, R. R. et al., 2009, Gorno-Tempini et al., 2011, Hodges, J. R. et al., 1992, Tan et al., 2014), in the perirhinal cortex (PRC), entorhinal cortex (ERC) and hippocampus (Chan et al., 2001, Davies, R. Rhys et al., 2009, Davies, R. R. et al., 2004, Galton et al., 2001). Studies investigating longitudinal atrophy rates generally match these findings, reporting significantly greater atrophy rates in the anterior temporal lobes in svPPA compared to controls (Frings et al., 2012, Krueger et al., 2010, Lam et al., 2014, Rogalski, E. et al., 2011, Rohrer, Jonathan D. et al., 2012), often more pronounced in the left hemisphere, although more pronounced atrophy rates in the right hemisphere have also been reported (Rohrer, J. D. et al., 2008).

However, most of these studies, especially the longitudinal ones, report coarse, global measures using standard resolution T1-weighted MRI (~1 mm isotropic). T2-weighted MRI with high in-plane resolution enables better measurement of MTL regions compared to T1-weighted MRI because of the clear visualization of 1) the stratum radiatum lacunosum moleculare in the hippocampus which makes up a considerable portion of the subfield borders in the hippocampus which can rarely be visualized on standard resolution T1-weighted MRI and 2) the dura adjacent to the MTL cortices which can be difficult to separate from the cortex on T1-weighted MRI. We hypothesize that granular assessment of atrophy in subfields of medial temporal lobe (MTL) regions, such as hippocampal subfields and perirhinal subregions (Brodmann areas (BA) 35 and 36), using T2-weighted MRI can provide a better characterization of the topography and degree of subregional MTL atrophy in svPPA. Indeed, several previous studies indicated that high resolution T2-weighted MRI approached outperformed T1-weighted MRI approaches in the detection of early stage atrophy in AD, β-amyloid positivity, cognitive associations and in sample size calculation for detecting change in patients' atrophy rates compared to controls (Das, S. R. et al., 2012, de Flores, La Joie, Landeau et al., 2015, Mueller et al., 2018).

MTL atrophy patterns can potentially provide insight into the underlying pathology, as MTL subregions are thought to be differentially vulnerable to different pathologies such as 43-kDa TAR DNA-binding protein (TDP-43) (Brettschneider et al., 2014), which is thought to underlie svPPA in the majority of cases (Bonner, M. F. et al., 2010, Grossman, 2010, Mesulam et al., 2014, Spinelli et al., 2017). A better characterization of the topography of atrophy in MTL subregions thus could potentially be helpful in detecting the presence of TDP-43 pathology in individuals with MTL atrophy without dementia or another neurodegenerative disease (Josephs, Keith A. et al., 2019, Nag et al., 2018, Nelson, Peter et al., 2019). Although MTL atrophy is often associated with neurofibrillary tangle pathology in AD (Braak, H. and Braak, 1991), recent autopsy studies of AD emphasize the important role of TDP-43 co-pathology in hippocampal volume loss even in individuals with significant AD pathology (Josephs, Keith A. et al., 2017, Nelson, P. T. et al., 2013).

We are aware of only one previous study that assessed *hippocampal subfield* volumetry using T2-weighted MRI and showed that patients with svPPA have significantly smaller volumes of the subregions cornu ammonis (CA) 1 and subiculum compared to controls, suggesting specificity for these subfields (La Joie, Renaud et al., 2013). However, this study did not investigate adjacent MTL cortical regions (such as BA35 and BA36) or investigate longitudinal atrophy rates. Atrophy rates of MTL subfields could potentially provide better biomarkers to track disease progression or as endpoints in clinical trials. We therefore aim to investigate the MTL subregional atrophy pattern cross-sectionally and longitudinally in patients with svPPA as compared to controls and a dementia reference group, patients with AD. Besides hippocampal subfields CA1, subiculum and dentate gyrus (DG), we also interrogate aggregated anterior and posterior hippocampal regions. We hypothesize most pronounced atrophy, both cross-sectionally and longitudinally, in BA35 and BA36 in svPPA compared to controls and more so in the left than the right hemisphere, as well as more anterior than posterior hippocampal atrophy. Finally, we hypothesize that MTL atrophy in svPPA in the left hemisphere will be significantly greater than in AD.

While our paper is mainly focused on svPPA, we also interrogate cross-sectional and longitudinal MTL atrophy patterns in amnesic AD patients. It should be noted that approximately 80% of our AD patients had an early onset (i.e. before 65 years), in order to match the age of the svPPA patients. While MTL atrophy has been well demonstrated in late-onset AD (de Flores, La Joie and Chetelat, 2015), there have been few studies examining MTL atrophy that focus on AD patients with an earlier onset (Phillips et al., 2018), and we are unaware of investigations of MTL subfield atrophy in early-onset AD using T2-weighted imaging.

It has been hypothesized that tau pathology may originate in a different location in some non-amnesic cases of early AD, however, all AD patients included in this study had amnesic AD. Moreover, a recent neuropathology study showed that the subset of AD patients with an amnesic syndrome who on average had an age of onset of 62.6 years, had a median Braak stage of VI and significantly more NFT pathology in the subiculum compared to the cognitively impaired/mild dementia cases (Petersen et al., 2019), indicating that these cases harbor MTL NFT pathology. Our expectation is therefore that we will see neurodegeneration in the typical Braak regions in these early-onset amnesic cases of AD, including BA35

(approximates the transentorhinal cortex), ERC and CA1 (Braak, E. and Braak, 1997). We do not expect any differences between the hemispheres nor in anterior vs posterior hippocampal atrophy in AD.

Methods

Participants

Patients were recruited at the Penn Frontotemporal Degeneration (FTD) Center and Cognitive Neurology Clinic at the University of Pennsylvania. For the current study only patients with a diagnosis of svPPA or early onset AD and with available T1- and T2-weighted MRI scans were selected. A diagnosis of svPPA was established by a board-certified neurologist based upon published criteria (Gorno-Tempini et al., 2011) and a neuropsychological profile consistent with svPPA. The clinical diagnosis was based on clinical criteria and then image-supported when clinical imaging was available (note that the high resolution T2-weighted MRI scans were not used to support the clinical diagnosis). Out of 15 svPPA patients, 14 had available cerebrospinal fluid (CSF) measures of tau and β-amyloid (Aβ). Most showed a tau-to-Aβ ratio of <0.34 consistent with non-AD pathology (Irwin et al., 2012), although two patients with svPPA had a CSF tau-to-Aβ ratio which was marginally above the cut off of >0.34 (0.38 and 0.41). Many patients underwent neuropsychological examination with the Unified Data Set – 2 (UDS-2) and more recent cases also underwent the FTLD-National Alzheimer's Coordination Center protocol which also included the neuropsychiatric inventory (see more details in the section Cognitive tasks). Moreover, all patients were evaluated for extrapyramidal and behavioral symptoms at every evaluation. Demographically-matched patients with a clinical diagnosis of AD were also recruited. The clinical diagnosis of AD was established according to the McKhann criteria (McKhann et al., 2011). All AD patients had an amnesic AD phenotype. Out of 59 patients with AD, six showed a tau-to-Aβ ratio of <0.34 and were excluded, thirteen did not have available CSF measures and two had CSF measures but more than 1.5 years after the MRI scan and were excluded, resulting in a cohort of 38 AD patients with CSF evidence of AD pathology obtained either close in time to the MRI scan or before the MRI scan. Additional exclusion criteria were any evidence of vascular disease, hydrocephalus, head trauma or other neurological disorder or medical illness that could affect cognition or a medication regimen that could affect cognition. Additionally, 24 cognitively normal older adults of similar age were selected from a panel of cognitively healthy volunteers, with no history of a medical condition or neurological disorder that could affect cognition. After quality assessment of the MRI scans and segmentations (see section Medial temporal lobe segmentation below), data from 15 patients with svPPA, 37 patients with early onset AD, and 23 healthy controls were available. Out of 37 patients with AD, 30 (81.1%) had an estimated age of onset 65 or younger and are therefore traditionally considered early onset AD, or EOAD. Moreover, the majority of the patients in the AD group had dementia, however, eight had Mild Cognitive Impairment (MCI).

A subset of patients, including 6 svPPA patients, 12 AD patients and 9 healthy controls, returned for a follow up MRI scan within 600 days after the initial scan. There were no significant differences between the patients and controls included in the longitudinal

analyses as compared to those not included on age, sex, education, disease duration and MMSE (P>0.05). Out of 12 patients with AD with longitudinal data, 10 (83.3%) had an estimated age of onset 65 or younger and are therefore considered EOAD. Additionally, out of 12 patients with AD, seven had MCI.

Standard protocol approvals, registrations and patient consents

The study was approved by the Institutional Review Board from the University of Pennsylvania and all participants provided written informed consent.

Data Availability

Anonymized data will be shared by request with any qualified investigator for purposes of validation and/or replication using our center's established methods for sharing data.

Cognitive tasks

While all subjects underwent cognitive testing, only a subset of the subjects underwent cognitive testing within 6 months of MRI scanning. Note that the data was collected over many years and as a result, different subsets of subjects completed each neuropsychological test. We chose to present neuropsychological tests that were available in the majority of the patients and that were most relevant for the two included patient groups, svPPA and amnesic AD. The Mini Mental Status Examination (MMSE) (Folstein et al., 1975) was obtained as well as specific tests for semantic and episodic memory. To assess semantic knowledge, the Boston Naming Task (BNT) (Kaplan et al., 1983) and the Pyramids and Palm Trees (PPT) test (Howard and Patterson, 1992) were used. For memory, delayed recall of the Philadelphia Verbal Learning Test (PVLT, (Libon et al., 1996)) and the 15-minute delayed recall of the Rey figure (Osterrieth, 1944) were obtained. To equate for differences in the total number of correct items across the BNT, PPT, delayed recall of the PVLT and Rey figure, the percentage of correct answers was calculated.

MR imaging

MRI scans were acquired at a 3T Siemens Tim Trio scanner. A high-resolution T2-weighted MRI scan, specialized for imaging the MTL, was acquired perpendicular to the long axis of the hippocampus with partial coverage, with a repetition time (TR) of 5310 ms, and echo time (TE) of 68 ms, a flip angle of 150°, a matrix size of 448×448, a voxel size of 0.4×0.4×2 mm^3 and a 0.6 mm gap, and an acquisition time of 7:01 min. Additionally, a T1-weighted MPRAGE scan was obtained with a TR of 1620 ms, an TE of 3.09 ms, a flip angle of 15°, a matrix size of 192×256, a voxel size of 0.97×0.97×1 mm^3 and an acquisition time of 5:11 min.

Medial temporal lobe subregion segmentation

The Automated Segmentation of Hippocampal Subfields software (Yushkevich et al., 2015) was used to obtain volumes CA1, CA2, CA3, DG, subiculum (SUB), ERC, BA35 and 36, which are subregions of the PRC, and the parahippocampal cortex (PHC) and an estimate of intracranial volume (ICV). The Dice Similarity Coefficient (DSC) comparing ASHS against the manual segmentation was higher than 0.70 for most of the subregions (Yushkevich et al.,

2015), except CA2 (0.552) and CA3 (0.525). For this reason, CA2 and CA3 were excluded from all analyses. Moreover, an anterior and posterior hippocampal region was created by merging all hippocampal subfield labels from ASHS and using the uncus as the border between anterior and posterior hippocampus (Malykhin et al., 2008). The volumes of cortical regions (ERC, BA35, BA36, PHC) were normalized by number of slices as recommended in (Yushkevich et al., 2015). ICV was regressed out for all volumes, based on the regression coefficients of the control group.

Quality assessment: All MRI scans and segmentations were visually inspected and the segmentations were edited if necessary. Decisions on quality of the segmentations were made separately for the left and the right hemisphere as well as separately for the hippocampus and the extrahippocampal regions to preserve as much data as possible. The quality assessment led to the exclusion of three left hemispheres and one right hemisphere for different svPPA patients, the left and right hemisphere of one healthy control subject and two left and one right hemisphere for AD patients as well as two left and right hippocampi and one left extrahippocampal region for AD patients. This leaves 15 svPPA patients (left: 12; right: 14), 38 AD patients (left: 36 (Hippocampus: 34, Extrahippocampal regions: 35); right: 37 (Hippocampus: 35, Extrahippocampal regions: 37)) and 23 cognitively normal controls (left: 23; right: 23). Segmentations were excluded when the segmentation was clearly inaccurate and could not be edited because the borders could not be identified either because of poor image quality or too severe atrophy.

Hemispheric asymmetry Index (HAI): For all subjects a HAI (La Joie, R. et al., 2013) was calculated by the following formula: HAI = ((Hippocampus_right − Hippocampus_left)/(Hippocampus_left + Hippocampus_right)) *100%. Positive values indicated smaller volumes in the left hemisphere compared to the right hemisphere. All svPPA patients had more pronounced left than right hemispheric atrophy, except for one subject. For the AD patients and elderly controls this was more of a mix, while on average these groups also had slightly smaller left than right hippocampal volumes. See Table 1 for the average HAI in each of the groups.

Anterior-to-posterior ratio: An anterior to posterior ratio was calculated as the percentage of the total hippocampus that is made up by the anterior hippocampus ((anterior hippocampal volume/total hippocampal volume) *100%) (La Joie, R. et al., 2013).

Longitudinal analyses: An unbiased deformation-based morphometry pipeline was used to estimate longitudinal change in MTL subregions (Das, Sandhitsu R. et al., 2012). This method is specifically optimized for measuring change from anisotropic T2-weighted MRI scans. All subjects passed quality assessment. First, percentage volume loss was calculated as follows: (Follow Up Subfield Volume − Baseline Subfield Volume)/Baseline Subfield volume * 100%. Second, to obtain annualized percentage volume loss, a correction was made for the slightly differing follow up times as follows: (Percentage volume change/follow up time in days)*365. The average time between the two scans was 382±151 days for the svPPA patients, 341±80 days for the AD patients and 399±52 days for the elderly controls (see also Supplementary Table 1).

Statistical analyses

Mann-Whitney U tests were performed to compare MTL subregion volumes and atrophy rates of the svPPA group to the healthy control group and the AD group, for the left and right hemisphere separately. No covariates were included as there were no significant differences between the groups in the potential confounders age, sex, disease duration (Table 1) and time difference between scans (Supplementary Table 1). A Wilcoxon Rank test was used to compare subregion volumes and atrophy rates between the left and the right hemisphere. Note that in the analyses looking at longitudinal atrophy rates or when comparing left and right hemispheres, MTL measures are not corrected for ICV as these are within-subject comparisons.

For each of the analyses we performed a multiple comparison correction using the Holm-Bonferroni method.

Results

Demographics

Cross-sectional dataset: The demographics of the groups are displayed in Table 1. There were no significant differences in age, sex and education between svPPA and the other groups, and no difference for disease duration between the two patient groups. None of the svPPA patients was an APOE-4 carrier, which was significantly different from the AD patients and at a trend level from the healthy controls.

Compared to the healthy controls, patients with svPPA had significantly decreased scores on the BNT, PPT and verbal delayed recall. Compared to the AD group, the svPPA group had significantly worse performance on the BNT but significantly better performance on the delayed recall task of the Rey figure. svPPA and AD groups were similarly impaired in their verbal delayed memory performance. Compared to the elderly controls, the AD group was impaired on all cognitive tests except the Rey figure recall. These findings are consistent with the clinical diagnoses of svPPA and AD.

Longitudinal dataset: Demographics of the longitudinal dataset are shown in Supplementary Table 1. There were no significant differences in age, sex, education and follow up time between the three groups, and no difference for disease duration between the two patient groups. The only observed difference was a significantly lower MMSE score in the AD group compared to the elderly control group and a qualitatively lower MMSE score in the svPPA group compared to the elderly control group.

Anterior and posterior hippocampal analyses

Cross-sectional analyses: Both left anterior and posterior hippocampal volumes are smaller in svPPA compared to controls and left anterior hippocampal volumes are also smaller compared to AD patients (Table 2). The left anterior-to-posterior ratio is also significantly different in svPPA compared to the other groups, indicating that the anterior hippocampus is relatively more affected than the posterior hippocampus in svPPA compared to the other groups.

In AD, both left and right anterior and posterior hippocampal volumes are smaller compared to those of healthy controls, however the ratio is not significantly different from that of healthy controls.

Longitudinal analyses: No significant differences were observed in anterior or posterior hippocampal atrophy rates for any of the group comparisons, after Holm-Bonferroni correction (Table 3). However, qualitatively left anterior and posterior hippocampal atrophy rates were more pronounced in the svPPA group, and posterior atrophy rates in the svPPA group were qualitatively slightly larger than anterior hippocampal atrophy rates.

MTL subregional analyses

Cross-sectional analyses: Representative cases of MTL subregional imaging in svPPA, healthy controls and AD are illustrated in Figure 1. Compared to healthy controls, svPPA patients had significantly smaller volumes of all left MTL regions and right CA1, BA35 and BA36. Other MTL regions in the right hemisphere were smaller than in healthy controls, but not to a significant extent (Table 4). Compared to the AD group, patients with svPPA had significantly smaller left CA1, BA35 and left and right BA36 volumes. There were no MTL subregions that were significantly smaller in AD than svPPA. Figure 2a illustrates that BA35 and BA36 show qualitatively the most pronounced atrophy, followed by CA1 in the left hemisphere. Figure 2b shows that the right hemisphere matches this pattern, although with less pronounced atrophy in BA35. Compared to the elderly control group, AD has significantly smaller left and right CA1, DG, BA35 and PHC volumes. Other regions are also qualitatively smaller but not to a significant degree.

Comparisons of MTL subregion volumes between the left and right hemisphere showed that every left hemisphere subregion was noticeably and significantly smaller than its right hemisphere homologue in the svPPA group. However, this did not survive Holm Bonferroni correction. The lack of significant differences in the svPPA group is likely due to a lack of power. Left and right hemisphere subregions were much more comparably sized in AD and control groups, except for significantly smaller left than right CA1 in the AD group (this survived Holm-Bonferroni correction).

Longitudinal analyses: Exploratory longitudinal analyses were performed in the smaller subset with available longitudinal data. Comparing atrophy rates in MTL regions of svPPA patients with the other groups, we found significantly increased longitudinal atrophy rates in left and right BA36 in svPPA patients compared to healthy controls (Table 5). However, qualitatively all regions showed noticeably greater atrophy rates in svPPA compared to healthy controls. Figure 2c and 2d show a fairly similar pattern longitudinally compared to the cross-sectional atrophy pattern for both hemispheres, although left SUB shows a more pronounced atrophy rate in svPPA. No significant differences in atrophy rates were found between patients with svPPA and patients with AD, although the atrophy rates were qualitatively greater in the svPPA group than the AD group for all but two regions. Left and right atrophy rates were not significantly different in any of the groups (data not shown). Again, this is likely due to a lack of power.

The AD group showed most pronounced atrophy rates in BA35 compared to the elderly control group which reached significance for the right hemisphere. Moreover, right BA36 atrophy rates were also significantly larger in AD patients compared to controls.

Additional analyses

Excluding the two svPPA patients with a CSF tau-to-abeta ratio >0.34 did not change the results. Moreover, one svPPA patient had relatively more pronounced right-sided atrophy, and excluding this patient did not change the results.

We also repeated the analyses without the AD patients with an estimated onset after 65 years and this did not change the results. Finally, we repeated the analyses for the AD group without the MCI patients and this did also not notably change the results.

Discussion

This study has several key findings. First, we found that svPPA has significant atrophy in all left and several right MTL subregions compared to healthy controls. Moreover, svPPA has significantly smaller left CA1, BA35 and left and right BA36 than AD, and all other left MTL regions were smaller than those in AD, although not to a significant extent. We also found more pronounced cross-sectional anterior than posterior hippocampal atrophy in svPPA compared to both AD and control comparison groups. Longitudinal analyses revealed that svPPA has a significantly faster rate of decline than healthy controls in left and right BA36 and had relatively more rapid decline in all other regions. Indeed, in all but two subregions, svPPA had a rate of declining atrophy that was more rapid than in AD, although not to a significant extent.

Strengths and limitations

A strength of our study is that we used high resolution T2-weighted images which allowed us to measure hippocampal subregions and to account for confounders such as the dura, which can be easily separated from grey matter on T2-weighted images but not on the more commonly used T1-weighted images. Moreover, we used a well-validated automated segmentation method with a segmentation scheme that was developed together with a neuroanatomist. Another strength of our study is its comparative design, using T2-weighted imaging to evaluate relative MTL atrophy in svPPA compared to AD. Finally, in the small number of cases with available data, we performed longitudinal analyses in svPPA as well as AD and controls. Several limitations should be taken into account when interpreting these findings. While our sample size for svPPA falls well within the range of those of previous studies (Davies, R. R. et al., 2009, Galton et al., 2001, Krueger et al., 2010, Rogalski, E. et al., 2011), the first limitation is the relatively small sample size of rare svPPA patients. This limited our power to detect group differences, and this was most apparent in our comparisons of left versus right MTL regions in svPPA, where all left hemisphere subregions were noticeably smaller than the right hemisphere homologues although not after Bonferroni correction. Second, the time between the two MRI scans was relatively short (~1 year) which may have made our atrophy rate estimations less stable and may have limited our power to detect significant differences in atrophy rates between the groups. Third, there

was sometimes limited grey-white matter contrast in the MRI scans of the svPPA patients, especially in the more severe cases. We mitigated this as much as possible by careful quality assessment of the MRI scans and segmentations, and careful editing using both the T1- and T2-weighed MRI if needed. Fourth, in most of the healthy controls no CSF biomarkers of AD pathology were available. It is therefore possible that cross-sectional and longitudinal atrophy in the healthy controls may have been influenced by AD pathology. However, this likely would have led to an underestimation of the actual group differences and we believe that the results would likely have been stronger if the healthy controls are limited to a β-amyloid-negative group only. Fifth, our patient groups had on average 3 years of disease duration when first seen, and we were therefore not able to measure changes in the earliest stages of the disease. Moreover, estimates of disease duration have limitations related to the sensitivity of family members and loved ones to the presence of word-finding problems and comprehension difficulties, and it is therefore possible that some patients were in more advanced stages of the disease.

MTL atrophy patterns in svPPA

The cross-sectional findings are consistent with previous studies showing anterior MTL atrophy in svPPA using traditional T1-weighted imaging (Davies, R. R. et al., 2009, Gorno-Tempini et al., 2011, Hodges, J. R. et al., 1992, Tan et al., 2014), with most pronounced atrophy in the PRC (note that what we call BA35 and BA36 is sometimes included in the fusiform gyrus and the parahippocampal gyrus (Davies, R. Rhys et al., 2009, Davies, R. R. et al., 2004, Galton et al., 2001)) and more pronounced atrophy in the anterior rather than the posterior hippocampus (Chapleau et al., 2016, Davies, R. Rhys et al., 2005, La Joie, Renaud et al., 2013, Tan et al., 2014). Note that our longitudinal data revealed more pronounced atrophy in the posterior than anterior hippocampus, although not to a significant extent, potentially indicating plateauing of the atrophy rates of the anterior hippocampus.

While svPPA atrophy was more pronounced qualitatively in the PRC, atrophy was relatively widespread throughout the MTL in part because the svPPA patients included in this study had on average a disease duration of 3 years. It is likely that more specificity would be observed in earlier stages of the disease. Atrophy was more pronounced in every left hemisphere subregion compared to its right hemisphere homologue, although this is not significant following correction for multiple comparisons. While svPPA is typically characterized by more pronounced atrophy in the left hemisphere (Davies, R. R. et al., 2009, Gorno-Tempini et al., 2011, Hodges, J. R. et al., 1992, Tan et al., 2014), our study included one patient with more pronounced right-hemispheric atrophy (see also (Josephs, Keith Anthony et al., 2008, Thompson et al., 2003)). Additional studies are needed to understand these atypical cases.

At first sight, our results regarding hippocampal subfields seem to partly contrast with the only other study investigating these subfields on T2-weighted MRI (La Joie, Renaud et al., 2013), which reported most pronounced atrophy in CA1 and the subiculum, whereas we found that CA1 was qualitatively the most affected, followed by the DG and by the subiculum in both hemispheres. However, it is possible that differences in segmentation protocols may have caused these differences. Interestingly, our CA1/subiculum border is

more medial than in the La Joie et al. protocol in the hippocampal body (La Joie, R. et al., 2010) and thus includes a considerable portion of what is called subiculum in the La Joie et al. protocol. As our CA1 label includes both CA1 and a portion of the subiculum of the La Joie et al. study, the results may actually be very similar. Moreover, our findings match a post mortem study indicating more pronounced atrophy in CA1 than the DG (Davies, R. Rhys et al., 2005). Note that the subiculum was not assessed in that study.

While we have no pathological evidence of TDP-43 pathology in our svPPA group, it is the most common form of pathology in svPPA and this group therefore reflects “probable TDP-43”. Therefore, our findings suggest the sensitivity of the MTL to TDP-43 pathology, and this may also impact the MTL in Limbic-predominant Age-related TDP-43 Encephalopathy (LATE (Nelson, Peter et al., 2019)) and TDP-43 in the context of AD (Josephs, Keith A. et al., 2017). Additional work is needed to assess the rare subset of svPPA with primarily tau or AD pathology. Another potential factor related to MTL atrophy could be APOE-4 carrier status, which has been linked to MTL atrophy in the presence of AD pathology (Wolk et al., 2010). However, it is unlikely that APOE-4 carrier status can explain the observed MTL atrophy in svPPA in this study as none of the 10 svPPA patients with information on APOE status was an APOE-4 carrier.

Interestingly, several regions including left BA35 showed significantly more pronounced atrophy cross-sectionally in svPPA than AD, even though BA35, which approximates the transentorhinal cortex, is the earliest site of neurofibrillary tangle pathology (Braak, H. and Braak, 1991). While it is possible that the less pronounced atrophy in the AD group is due to the inclusion of several patients with MCI, this does not seem likely as the disease duration in both groups is similar and the MMSE score in the AD group is actually lower than the svPPA group. Moreover, repeating the analyses without the MCI patients did not change the results. Additionally, it should be noted that most patients with AD included in this study had early onset AD, who, while showing MTL atrophy compared to healthy controls, tend to have less MTL involvement compared to late onset AD (Cavedo et al., 2014, Cho et al., 2013, Frisoni, G. B. et al., 2005). The difference in BA35 atrophy between patients with AD and svPPA was most apparent in the left hemisphere, potentially reflecting the significantly greater naming impairment in svPPA than AD. Detailed clinical-anatomical studies also have associated the specific semantic impairment profile in svPPA for concrete object concepts with significant atrophy in these anterior temporal regions (Bonner, Michael F. et al., 2016, Cousins et al., 2016, Cousins et al., 2017). Likewise, visual memory was significantly less impaired in svPPA than AD, potentially reflecting a relatively spared right MTL in svPPA. The larger visual memory recall impairments in AD compared to svPPA could potentially be the result of more pronounced baseline atrophy in the right posterior hippocampus and PHC (significantly different from controls but not svPPA). In combination with other regions such as the posterior cingulate, typically atrophied in AD, these MTL regions together make up the posterior temporal system which is thought to subserve episodic recollection (Ranganath and Ritchey, 2012). Regardless of the consequences of lateralized disease in svPPA, the presence of significant MTL atrophy in association with TDP-43 pathology is consistent with the AT(N) (β-amyloid deposition, pathological tau and neurodegeneration) framework that neurodegenerative measures such as MRI atrophy have

limited specificity to underlying molecular pathology (Jack Jr et al., 2018, Knopman et al., 2018).

We observed most pronounced longitudinal atrophy rates in svPPA in left BA36, right BA35 and BA36 reaching between 8.52–9.02% volume loss/year. These rates of decline for these fine-grained MTL subregions are much larger than those reported for more global measures (1.6–2.6% volume loss/years (Gordon et al., 2010, Knopman et al., 2009), but are more similar to those reported for the temporal lobe (Frings et al., 2012, Krueger et al., 2010, Rogalski, Emily et al., 2014, Rohrer, Jonathan D. et al., 2012). Similar to previous longitudinal studies (Czarnecki et al., 2008, Frings et al., 2012, Krueger et al., 2010, Rogalski, Emily et al., 2014, Rohrer, Jonathan D. et al., 2012), the current study showed somewhat more pronounced atrophy in the left hemisphere (but note Rohrer et al. (Rohrer, J. D. et al., 2008) who reported more pronounced atrophy rates in the right hemisphere). We also observed considerable atrophy rates in the right hemisphere. This fits with the general notion that atrophy in svPPA spreads from the left to the right hemisphere over time (Marshall et al., 2018), potentially showing early involvement in the amygdala and the temporal pole in the MTL (Bocchetta et al., 2019). Another notable finding is that there are considerable differences in atrophy rates between the different MTL subregions. This indicates that subregion-specific information is lost in more global measures such as the temporal lobe or hippocampus and that subregional measures of decline might provide more sensitive and specific biomarkers for clinical trials, especially in the early stages when atrophy might still be very localized. Some evidence for this comes from detailed longitudinal clinical-anatomic studies of the declining semantic memory profile in svPPA, where a specific decline in concrete object knowledge is associated with progressive atrophy in the anterior temporal region (Cousins et al., 2018). However, our longitudinal analyses of MTL subfields using T2-weighted MRI need to be replicated in a larger sample.

MTL atrophy pattern in amnesic AD

While this study was mainly focused on MTL atrophy patterns in svPPA, we also investigated MTL atrophy patterns in a group of amnesic AD patients, of whom the majority had early onset AD. We found significant cross-sectional atrophy, bilaterally, in BA35 and CA1, but also in DG and PHC. Moreover, longitudinally, progressive atrophy was most pronounced in BA35 in both hemispheres in AD compared to healthy controls, even though this comparison only reached significance for the right hemisphere. Additionally, right BA36 atrophy rates were also larger in AD patients compared to healthy controls. While atrophy in BA35 and CA1 is in line with the expectations as early loci for NFT pathology (Braak, H. and Braak, 1991), cross-sectional volume loss in the DG and PHC and longitudinal atrophy rates in BA36 is perhaps less expected. It should be noted that these patients already had evidence of clinical AD for three years and perhaps NFT pathology had already spread to other MTL regions. A possible explanation for more pronounced atrophy rates in BA36 is that the boundaries with BA35 are difficult to determine and BA36 may have included some portion of BA35. However, as BA35 is smaller than BA36, this can likely not fully explain this finding. A possible explanation for the DG atrophy is that this label actually includes the stratum radiatum lacunosum moleculare (SRLM) in this atlas set (Yushkevich et al., 2015), and SRLM is actually an early target of NFT pathology (Adler et al., 2018, Braak, E. and

Braak, 1997, Kerchner et al., 2010, Thal et al., 2000). This inclusion of SRLM in the DG label perhaps partially explains the atrophy effects in the DG. A possible explanation for the atrophy observed in PHC is that PHC is part of the posterior MTL network (Ranganath and Ritchey, 2012), which is also thought to be affected in the early stages of AD (Das, S. R. et al., 2015) and especially by β-amyloid pathology (Schöll et al., 2016). As β-amyloid pathology has accrued over the years preceding the diagnosis in the posterior MTL network, this pathology may have indirectly affected the integrity of the PHC. As noted, atrophy in the posterior MTL network likely contributes in part to the episodic memory impairments, observed in this group. Although limited information is available about MTL subregional atrophy patterns in early amnesic AD, these findings are in line with previous studies reporting both cross-sectional and longitudinal atrophy in gross MTL regions in early and late onset AD with memory impairments (Cho et al., 2013, Frisoni, Giovanni B. et al., 2007).

Conclusions

This study revealed MTL subfield atrophy patterns in svPPA, with most pronounced atrophy in the PRC, in anterior regions of the MTL, and in the MTL of the left hemisphere. Significant progressive atrophy in BA36, part of the PRC, was observed over time. The considerable differences in atrophy rates between the different MTL subregions indicate that subregional measures of decline might provide more sensitive and specific biomarkers for clinical trials, especially in the early stages when atrophy might still be very localized. However, this should be further explored in future studies in larger samples sizes.

Supplementary Material

Refer to Web version on PubMed Central for supplementary material.

Study funding and acknowledgements

National Institutes of Health grants: AG056014, EB017255, AG010124, AG055005, AG017586, AG052943, AG054519, and AG066597.

References

Adler DH, Wisse LE, Ittyerah R, Pluta JB, Ding S, Xie L, Wang J, Kadivar S, Robinson JL, Schuck T, 2018. Characterizing the human hippocampus in aging and Alzheimer's disease using a computational atlas derived from ex vivo MRI and histology 115, 4252–4257.

Alladi S, Xuereb J, Bak T, Nestor P, Knibb J, Patterson K, Hodges JR, 2007. Focal cortical presentations of Alzheimer's disease 130, 2636–2645.

Bocchetta M, Iglesias JE, Russell LL, Greaves CV, Marshall CR, Scelsi MA, Cash DM, Ourselin S, Warren JD, Rohrer JD, 2019. Segmentation of medial temporal subregions reveals early right-sided involvement in semantic variant PPA 11, 41.

Bonner MF, Ash S, Grossman M, 2010. The new classification of primary progressive aphasia into semantic, logopenic, or nonfluent/agrammatic variants. Curr.Neurol.Neurosci.Rep 10, 484–490. [PubMed: 20809401]

Bonner MF, Price AR, Peelle JE, Grossman M, 2016. Semantics of the visual environment encoded in parahippocampal cortex. J.Cogn.Neurosci 28, 361–378. [PubMed: 26679216]

Braak E, Braak H, 1997. Alzheimer's disease: transiently developing dendritic changes in pyramidal cells of sector CA1 of the Ammon's horn. Acta Neuropathol 93, 323–325. [PubMed: 9113196]

Braak H, Braak E, 1991. Neuropathological stageing of Alzheimer-related changes. Acta Neuropathol 82, 239–259. [PubMed: 1759558]

Brettschneider J, Del Tredici K, Irwin DJ, Grossman M, Robinson JL, Toledo JB, Fang L, Van Deerlin VM, Ludolph AC, Lee VM, Braak H, Trojanowski JQ, 2014. Sequential distribution of pTDP-43 pathology in behavioral variant frontotemporal dementia (bvFTD). Acta Neuropathol 127, 423–439. [PubMed: 24407427]

Cavedo E, Pievani M, Boccardi M, Galluzzi S, Bocchetta M, Bonetti M, Thompson PM, Frisoni GB, 2014. Medial temporal atrophy in early and late-onset Alzheimer's disease. Neurobiol.Aging 35, 2004–2012. [PubMed: 24721821]

Chan D, Fox NC, Scahill RI, Crum WR, Whitwell JL, Leschziner G, Rossor AM, Stevens JM, Cipolotti L, Rossor MN, 2001. Patterns of temporal lobe atrophy in semantic dementia and Alzheimer's disease. Ann.Neurol 49, 433–442. [PubMed: 11310620]

Chapleau M, Aldebert J, Montembeault M, Brambati SM, 2016. Atrophy in Alzheimer's disease and semantic dementia: an ALE meta-analysis of voxel-based morphometry studies. J.Alzheimer's Dis 54, 941–955. [PubMed: 27567843]

Cho H, Jeon S, Kang SJ, Lee J, Lee J, Kim GH, Shin JS, Kim CH, Noh Y, Im K, 2013. Longitudinal changes of cortical thickness in early-versus late-onset Alzheimer's disease. Neurobiol.Aging 34, 1921. e9–1921. e15.

Cousins KA, Ash S, Irwin DJ, Grossman M, 2017. Dissociable substrates underlie the production of abstract and concrete nouns. Brain Lang 165, 45. [PubMed: 27912073]

Cousins KA, Ash S, Olm CA, Grossman M, 2018. Longitudinal changes in semantic concreteness in semantic variant Primary Progressive Aphasia (svPPA) 5.

Cousins KA, York C, Bauer L, Grossman M, 2016. Cognitive and anatomic double dissociation in the representation of concrete and abstract words in semantic variant and behavioral variant frontotemporal degeneration 84, 244–251.

Czarnecki K, Duffy JR, Nehl CR, Cross SA, Molano JR, Jack CR, Shiung MM, Josephs KA, Boeve BF, 2008. Very early semantic dementia with progressive temporal lobe atrophy: an 8-year longitudinal study. Arch.Neurol 65, 1659–1663. [PubMed: 19064755]

Das SR, Avants BB, Pluta J, Wang H, Suh JW, Weiner MW, Mueller SG, Yushkevich PA, 2012. Measuring longitudinal change in the hippocampal formation from in vivo high-resolution T2-weighted MRI. Neuroimage

Das SR, Pluta J, Mancuso L, Kliot D, Yushkevich PA, Wolk DA, 2015. Anterior and posterior MTL networks in aging and MCI. Neurobiol.Aging 36 Suppl 1, S141–50, S150.e1. [PubMed: 25444600]

Das SR, Avants BB, Pluta J, Wang H, Suh JW, Weiner MW, Mueller SG, Yushkevich PA, 2012. Measuring longitudinal change in the hippocampal formation from in vivo high-resolution T2-weighted MRI. Neuroimage 60, 1266–1279. [PubMed: 22306801]

Davies RR, Halliday GM, Xuereb JH, Kril JJ, Hodges JR, 2009. The neural basis of semantic memory: Evidence from semantic dementia. Neurobiol.Aging 30, 2043–2052. [PubMed: 18367294]

Davies RR, Hodges JR, Kril JJ, Patterson K, Halliday GM, Xuereb JH, 2005. The pathological basis of semantic dementia 128, 1984–1995.

Davies RR, Graham KS, Xuereb JH, Williams GB, Hodges JR, 2004. The human perirhinal cortex and semantic memory. Eur.J.Neurosci 20, 2441–2446. [PubMed: 15525284]

Davies RR, Halliday GM, Xuereb JH, Kril JJ, Hodges JR, 2009. The neural basis of semantic memory: evidence from semantic dementia. Neurobiol.Aging 30, 2043–2052. [PubMed: 18367294]

de Flores R, La Joie R, Chetelat G, 2015. Structural imaging of hippocampal subfields in healthy aging and Alzheimer's disease 309, 29–50.

de Flores R, La Joie R, Landeau B, Perrotin A, Mezenge F, de La Sayette V, Eustache F, Desgranges B, Chetelat G, 2015. Effects of age and Alzheimer's disease on hippocampal subfields: comparison between manual and FreeSurfer volumetry. Hum.Brain Mapp 36, 463–474. [PubMed: 25231681]

Folstein MF, Folstein SE, McHugh PR, 1975. "Mini-mental state". A practical method for grading the cognitive state of patients for the clinician. J.Psychiatr.Res 12, 189–198. [PubMed: 1202204]

Frings L, Mader I, Landwehrmeyer BG, Weiller C, Hüll M, Huppertz H, 2012. Quantifying change in individual subjects affected by frontotemporal lobar degeneration using automated longitudinal MRI volumetry. Hum.Brain Mapp 33, 1526–1535. [PubMed: 21618662]

Frisoni GB, Testa C, Sabattoli F, Beltramello A, Soininen H, Laakso MP, 2005. Structural correlates of early and late onset Alzheimer's disease: voxel based morphometric study 76, 112–114.

Frisoni GB, Pievani M, Testa C, Sabattoli F, Bresciani L, Bonetti M, Beltramello A, Hayashi KM, Toga AW, Thompson PM, 2007. The topography of grey matter involvement in early and late onset Alzheimer's disease 130, 720–730.

Galton CJ, Patterson K, Graham K, Lambon-Ralph MA, Williams G, Antoun N, Sahakian BJ, Hodges JR, 2001. Differing patterns of temporal atrophy in Alzheimer's disease and semantic dementia 57, 216–225.

Gordon E, Rohrer JD, Kim LG, Omar R, Rossor MN, Fox NC, Warren JD, 2010. Measuring disease progression in frontotemporal lobar degeneration: a clinical and MRI study 74, 666–673.

Gorno-Tempini ML, Hillis AE, Weintraub S, Kertesz A, Mendez M, Cappa SF, Ogar JM, Rohrer JD, Black S, Boeve BF, Manes F, Dronkers NF, Vandenberghe R, Rascovsky K, Patterson K, Miller BL, Knopman DS, Hodges JR, Mesulam MM, Grossman M, 2011. Classification of primary progressive aphasia and its variants 76, 1006–1014.

Grossman M, 2010. Primary progressive aphasia: clinicopathological correlations. Nat.Rev.Neurol 6, 88–97. [PubMed: 20139998]

Hodges JR, Patterson K, Oxbury S, Funnell E, 1992. Semantic dementia. Progressive fluent aphasia with temporal lobe atrophy. Brain 115 (Pt 6), 1783–1806. [PubMed: 1486461]

Hodges JR, Patterson K, 2007. Semantic dementia: a unique clinicopathological syndrome 6, 1004–1014.

Howard D, Patterson K, 1992. The Pyramids and Palm Trees Test: A test of semantic access from words and pictures. Pearson Assessment

Irwin DJ, McMillan CT, Toledo JB, Arnold SE, Shaw LM, Wang L, Van Deerlin V, Lee VM, Trojanowski JQ, Grossman M, 2012. Comparison of cerebrospinal fluid levels of tau and Aβ 1–42 in Alzheimer disease and frontotemporal degeneration using 2 analytical platforms. Arch.Neurol 69, 1018–1025. [PubMed: 22490326]

Jack CR Jr, Bennett DA, Blennow K, Carrillo MC, Dunn B, Haeberlein SB, Holtzman DM, Jagust W, Jessen F, Karlawish J, 2018. NIA-AA Research Framework: Toward a biological definition of Alzheimer's disease 14, 535–562.

Josephs KA, Dickson DW, Tosakulwong N, Weigand SD, Murray ME, Petrucelli L, Liesinger AM, Senjem ML, Spychalla AJ, Knopman DS, 2017. Rates of hippocampal atrophy and presence of post-mortem TDP-43 in patients with Alzheimer's disease: a longitudinal retrospective study 16, 917–924.

Josephs KA, Hodges JR, Snowden JS, Mackenzie IR, Neumann M, Mann DM, Dickson DW, 2011. Neuropathological background of phenotypical variability in frontotemporal dementia. Acta Neuropathol 122, 137–153. [PubMed: 21614463]

Josephs KA, Murray ME, Tosakulwong N, Weigand SD, Serie AM, Perkerson RB, Matchett BJ, Jack CR, Knopman DS, Petersen RC, 2019. Pathological, imaging and genetic characteristics support the existence of distinct TDP-43 types in non-FTLD brains. Acta Neuropathol 137, 227–238. [PubMed: 30604226]

Josephs KA, Whitwell JL, Vemuri P, Senjem ML, Boeve BF, Knopman DS, Smith GE, Ivnik RJ, Petersen RC, Jack CR, 2008. The anatomic correlate of prosopagnosia in semantic dementia 71, 1628–1633.

Kaplan E, Goodglass H, Weintraub S, 1983. The Boston Naming Test Lea and Febiger, Philadelphia.

Kerchner GA, Hess CP, Hammond-Rosenbluth KE, Xu D, Rabinovici GD, Kelley DA, Vigneron DB, Nelson SJ, Miller BL, 2010. Hippocampal CA1 apical neuropil atrophy in mild Alzheimer disease visualized with 7-T MRI 75, 1381–1387.

Knopman DS, Haeberlein SB, Carrillo MC, Hendrix JA, Kerchner G, Margolin R, Maruff P, Miller DS, Tong G, Tome MB, 2018. The National Institute on Aging and the Alzheimer's Association Research Framework for Alzheimer's disease: perspectives from the research roundtable 14, 563–575.

Knopman DS, Jack CR, Kramer JH, Boeve BF, Caselli RJ, Graff-Radford NR, Mendez MF, Miller BL, Mercaldo ND, 2009. Brain and ventricular volumetric changes in frontotemporal lobar degeneration over 1 year 72, 1843–1849.

Krueger CE, Dean DL, Rosen HJ, Halabi C, Weiner M, Miller BL, Kramer JH, 2010. Longitudinal rates of lobar atrophy in frontotemporal dementia, semantic dementia, and Alzheimer's disease. Alzheimer Dis.Assoc.Disord 24, 43. [PubMed: 19571735]

La Joie R, Fouquet M, Mezenge F, Landeau B, Villain N, Mevel K, Pelerin A, Eustache F, Desgranges B, Chetelat G, 2010. Differential effect of age on hippocampal subfields assessed using a new high-resolution 3T MR sequence. Neuroimage 53, 506–514. [PubMed: 20600996]

La Joie R, Perrotin A, de La Sayette V, Egret S, Doeuvre L, Belliard S, Eustache F, Desgranges B, Chetelat G, 2013. Hippocampal subfield volumetry in mild cognitive impairment, Alzheimer's disease and semantic dementia. Neuroimage Clin 3, 155–162. [PubMed: 24179859]

La Joie R, Perrotin A, Sayette d.L., Egret S, Doeuvre L, Belliard S, Eustache F, Desgranges B, Chetelat G, 2013. Hippocampal subfield volumetry in mild cognitive impairment, Alzheimer's disease and semantic dementia. NeuroImage: Clinical 3, 155–162. [PubMed: 24179859]

Lam BY, Halliday GM, Irish M, Hodges JR, Piguet O, 2014. Longitudinal white matter changes in frontotemporal dementia subtypes. Hum.Brain Mapp 35, 3547–3557. [PubMed: 25050433]

Libon DJ, Mattson RE, Glosser G, Kaplan E, Malamut BL, Sands LP, Swenson R, Cloud BS, 1996. A nine—word dementia version of the California verbal learning test. Clin.Neuropsychol 10, 237–244.

Malykhin NV, Bouchard TP, Camicioli R, Coupland NJ, 2008. Aging hippocampus and amygdala 19, 543–547.

Marshall CR, Hardy CJ, Volkmer A, Russell LL, Bond RL, Fletcher PD, Clark CN, Mummery CJ, Schott JM, Rossor MN, 2018. Primary progressive aphasia: a clinical approach. J.Neurol 265, 1474–1490. [PubMed: 29392464]

McKhann GM, Knopman DS, Chertkow H, Hyman BT, Jack CR Jr, Kawas CH, Klunk WE, Koroshetz WJ, Manly JJ, Mayeux R, Mohs RC, Morris JC, Rossor MN, Scheltens P, Carrillo MC, Thies B, Weintraub S, Phelps CH, 2011. The diagnosis of dementia due to Alzheimer's disease: recommendations from the National Institute on Aging-Alzheimer's Association workgroups on diagnostic guidelines for Alzheimer's disease. Alzheimers Dement 7, 263–269. [PubMed: 21514250]

Mesulam M, Weintraub S, Rogalski EJ, Wieneke C, Geula C, Bigio EH, 2014. Asymmetry and heterogeneity of Alzheimer's and frontotemporal pathology in primary progressive aphasia 137, 1176–1192.

Mueller SG, Yushkevich PA, Das S, Wang L, Van Leemput K, Iglesias JE, Alpert K, Mezher A, Ng P, Paz K, 2018. Systematic comparison of different techniques to measure hippocampal subfield volumes in ADNI2 17, 1006–1018.

Nag S, Yu L, Boyle PA, Leurgans SE, Bennett DA, Schneider JA, 2018. TDP-43 pathology in anterior temporal pole cortex in aging and Alzheimer's disease 6, 33.

Nelson PT, Smith CD, Abner EL, Wilfred BJ, Wang WX, Neltner JH, Baker M, Fardo DW, Kryscio RJ, Scheff SW, Jicha GA, Jellinger KA, Van Eldik LJ, Schmitt FA, 2013. Hippocampal sclerosis of aging, a prevalent and high-morbidity brain disease. Acta Neuropathol 126, 161–177. [PubMed: 23864344]

Nelson P, Dickson D, Trokanowski J, Jack C Jr, Boyle P, Arfanakis K, Rademakers R, Alafuzoff I, Attems J, Brayne C, 2019. Limbic-predominant Age-related TDP-43 Encephalopathy (LATE): Consensus Working Group Report

Osterrieth PA, 1944. Filetest de copie d'une figure complex: Contribution a l'etude de la perception et de la memoire. Archives de Psychologie 30, 286–365.

Petersen C, Nolan AL, Resende Elisa de Paula FranÃ§a, Miller Z, Ehrenberg AJ, Gorno-Tempini ML, Rosen HJ, Kramer JH, Spina S, Rabinovici GD, 2019. Alzheimer's disease clinical variants show distinct regional patterns of neurofibrillary tangle accumulation. Acta Neuropathol 138, 597–612. [PubMed: 31250152]

Phillips JS, Da Re F, Dratch L, Xie SX, Irwin DJ, McMillan CT, Vaishnavi SN, Ferrarese C, Lee EB, Shaw LM, 2018. Neocortical origin and progression of gray matter atrophy in nonamnestic Alzheimer's disease. Neurobiol.Aging 63, 75–87. [PubMed: 29223682]

Ranganath C, Ritchey M, 2012. Two cortical systems for memory-guided behaviour 13, 713–726.

Rogalski E, Cobia D, Harrison TM, Wieneke C, Weintraub S, Mesulam M, 2011. Progression of language decline and cortical atrophy in subtypes of primary progressive aphasia 76, 1804–1810.

Rogalski E, Cobia D, Martersteck A, Rademaker A, Wieneke C, Weintraub S, Mesulam M, 2014. Asymmetry of cortical decline in subtypes of primary progressive aphasia 83, 1184–1191.

Rohrer JD, McNaught E, Foster J, Clegg SL, Barnes J, Omar R, Warrington EK, Rossor MN, Warren JD, Fox NC, 2008. Tracking progression in frontotemporal lobar degeneration: serial MRI in semantic dementia 71, 1445–1451.

Rohrer JD, Clarkson MJ, Kittus R, Rossor MN, Ourselin S, Warren JD, Fox NC, 2012. Rates of hemispheric and lobar atrophy in the language variants of frontotemporal lobar degeneration. J.Alzheimer's Dis 30, 407–411. [PubMed: 22406442]

Schöll M, Lockhart SN, Schonhaut DR, Oâ€™Neil JP, Janabi M, Ossenkoppele R, Baker SL, Vogel JW, Faria J, Schwimmer HD, 2016. PET imaging of tau deposition in the aging human brain 89, 971–982.

Spinelli EG, Mandelli ML, Miller ZA, Santos-Santos MA, Wilson SM, Agosta F, Grinberg LT, Huang EJ, Trojanowski JQ, Meyer M, 2017. Typical and atypical pathology in primary progressive aphasia variants. Ann.Neurol 81, 430–443. [PubMed: 28133816]

Tan RH, Wong S, Kril JJ, Piguet O, Hornberger M, Hodges JR, Halliday GM, 2014. Beyond the temporal pole: limbic memory circuit in the semantic variant of primary progressive aphasia 137, 2065–2076.

Thal DR, Holzer M, Rub U, Waldmann G, Gunzel S, Zedlick D, Schober R, 2000. Alzheimer-related tau-pathology in the perforant path target zone and in the hippocampal stratum oriens and radiatum correlates with onset and degree of dementia. Exp.Neurol 163, 98–110. [PubMed: 10785448]

Thompson SA, Patterson K, Hodges JR, 2003. Left/right asymmetry of atrophy in semantic dementia: behavioral–cognitive implications 61, 1196–1203.

Wolk DA, Dickerson BC, Alzheimerâ€™s Disease Neuroimaging Initiative, 2010. Apolipoprotein E (APOE) genotype has dissociable effects on memory and attentionalâ€“executive network function in Alzheimerâ€™s disease. 107, 10256–10261.

Yushkevich PA, Pluta JB, Wang H, Xie L, Ding SL, Gertje EC, Mancuso L, Kliot D, Das SR, Wolk DA, 2015. Automated volumetry and regional thickness analysis of hippocampal subfields and medial temporal cortical structures in mild cognitive impairment. Hum.Brain Mapp 36, 258–287. [PubMed: 25181316]

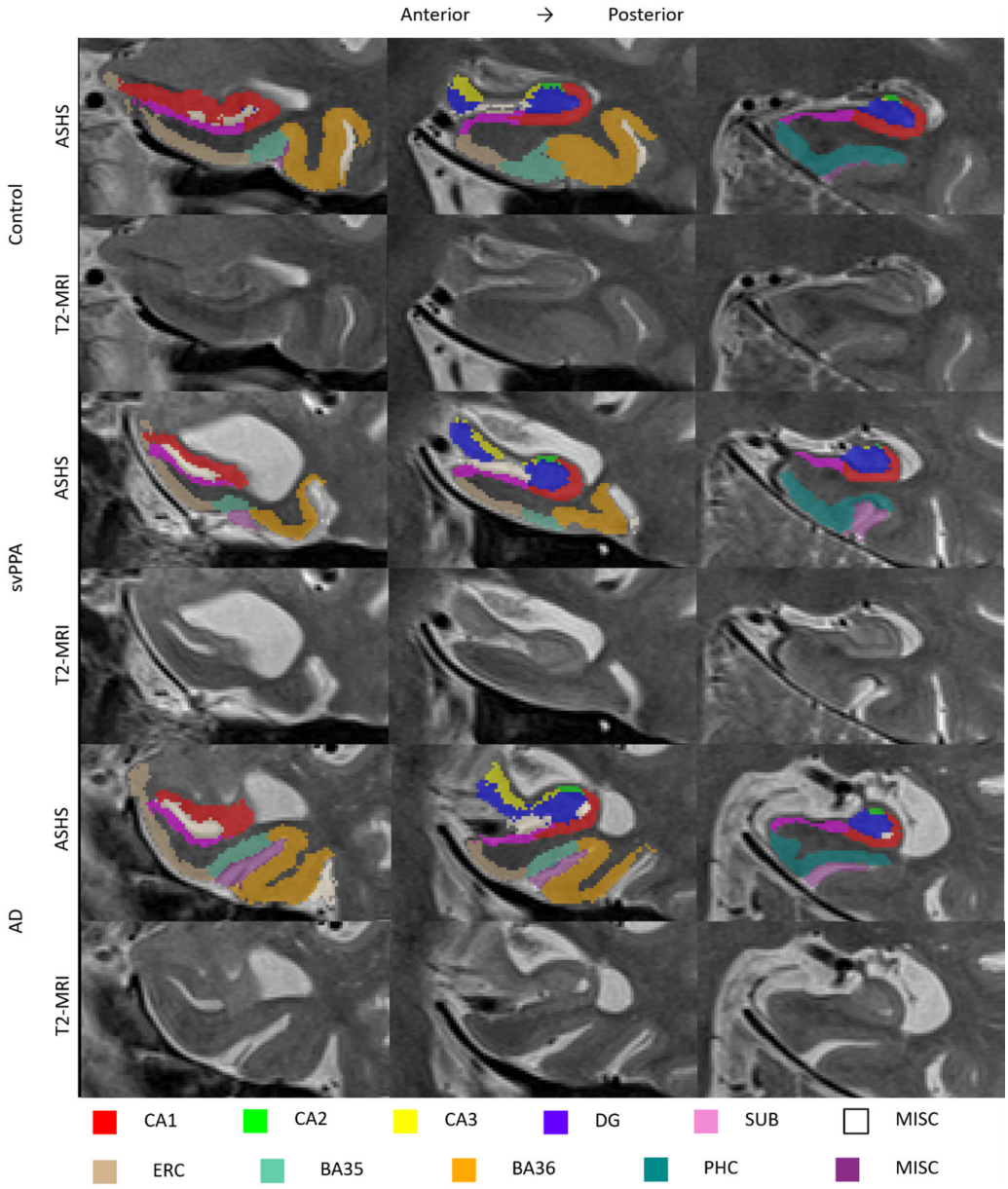

Figure 1.

T2-weighted MRI (lower panel) and accompanying MTL subregion segmentation (upper panel) for a representative svPPA, healthy control and AD case

ASHS=Automated Segmentation of Hippocampal Subfields; CA=cornu ammonis; DG=dentate gyrus; SUB=subiculum; MISC=miscellaneous ERC=entorhinal cortex; BA=Brodmann area; PHC=parahippocampal cortex

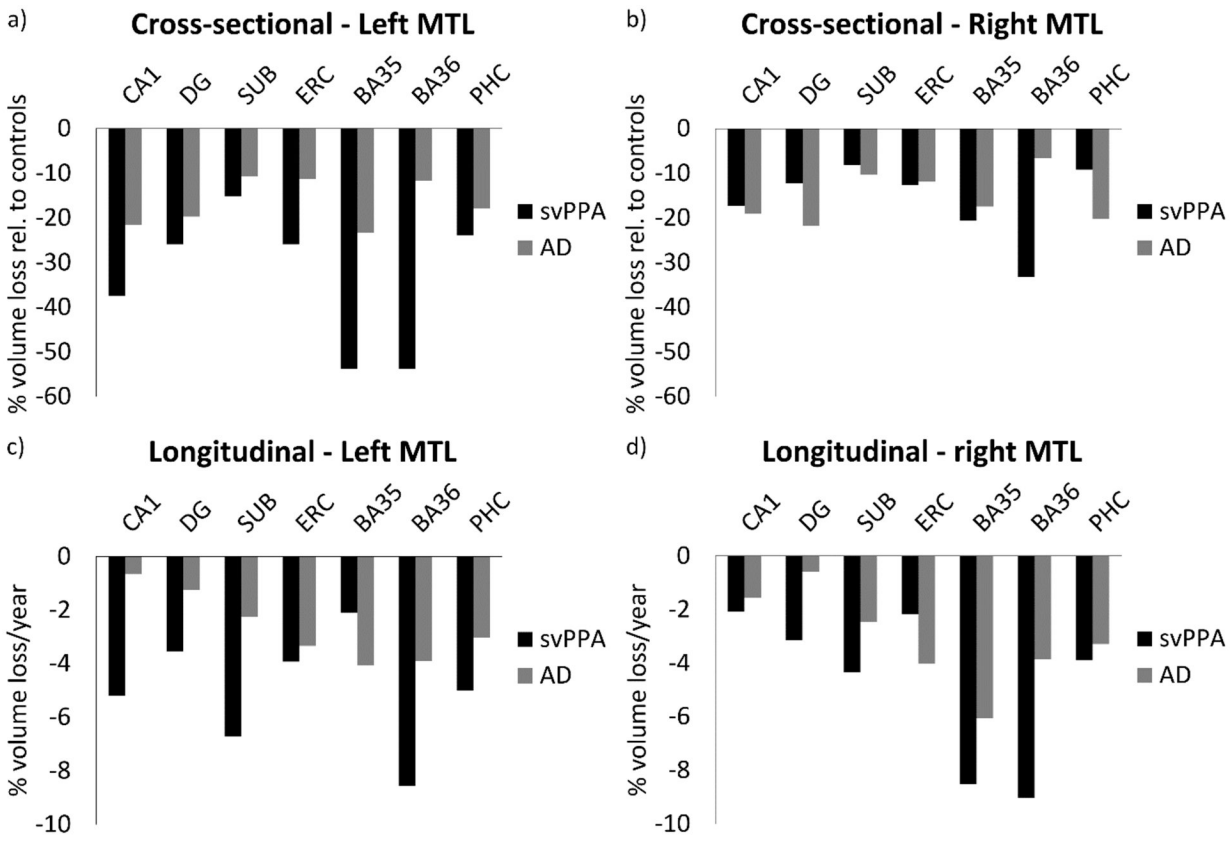

Figure 2.

Cross-sectional (a, b) and longitudinal (c, d) atrophy patterns in the MTL in patients with svPPA and AD. Cross-sectional atrophy is expressed as percentage volume loss compared to the healthy controls.

svPPA=semantic variant Primary Progressive Aphasia; AD=Alzheimer's disease; CA=cornu ammonis; DG=dentate gyrus; SUB=subiculum; ERC=entorhinal cortex; BA=Brodmann area; PHC=parahippocampal cortex

Table 1.

Demographic and clinical features of svPPA, healthy controls and AD

	svPPA	Healthy control	svPPA vs control	AD	svPPA vs AD	AD vs control
	Mean±SD	**Mean±SD**	**p-value**	**Mean±SD**	**p-value**	**p-value**
N	15	23		37		
Age (years) (range) (total n)	63.1±7.3 (49–75) (15)	63.7±6.4 (55–76) (23)	0.836	61.6±8.2(49–82) (37)	0.368	0.204
Sex (% male) (total n)	66.7 (15)	60.9 (23)	0.717	48.6 (37)	0.238	0.356
Education (years) (total n)	17.2±2.5 (14)	16.0±2.3 (23)	0.313	15.9±2.7 (36)	0.145	0.733
Disease duration (years) (total n)	2.6±1.9 (15)	-	-	2.9±2.3 (37)	0.842	-
APOE-4 status (%) (total n)	0 (11)	13 (10)	0.050	54.1 (37)	**0.001**	0.177
One allele (% of APOE-4)[a]	0	66.7		80.0		
Two alleles (% of APOE-4)[a]	0	33.3		20.0		
CSF tau-to-abeta ratio (total n)	0.22±0.09 (14)	-	-	0.83±0.41 (37)	**<0.001**	-
HAI (total n)	10.65±9.74 (11)	1.43±2.35 (23)	**<0.001**	2.37±5.59 (33)	**<0.001**	0.335
MMSE (total n)	22.9±8.7 (14)	29.4±0.8 (14)	0.004	18.8±5.3 (33)	0.026	**<0.001**
BNT (% correct) (total n)	24.5±22.7 (12)	96.2±4.2 (18)	**<0.001**	66.4±25.3 (31)	**<0.001**	**<0.001**
PPT (% correct) (total n)	75.2±14.9 (6)	98.6±2.4 (7)	**0.001**	89.4±7.6 (13)	0.029	**0.001**
PVLT 9 (% correct) (total n)	32.2±25.4 (10)	88.9±15.7 (5)	**0.001**	22.6±22.7 (27)	0.286	**<0.001**
Rey Recall (% correct) (total n)	45.8±25.5 (10)	53.1±32.8 (5)	0.594	16.1±15.5 (25)	**0.001**	0.031

*Bolded values are significant after the Holm-Bonferroni correction.

[a]Number alleles were displayed for descriptive purposes, no statistics were performed. svPPA=semantic variant Primary Progressive Aphasia; AD=Alzheimer's disease; CSF=cerebrospinal fluid; HAI=Hemispheric Assymetry Index; MMSE=mini mental state examination; BNT=Boston naming task; PPT=Pyramids and Palm Trees Test; PVLT=Pennsylvania verbal learning task

Table 2.

Comparison of svPPA with healthy controls and AD on anterior and posterior hippocampal volumes (in mm^3; ICV is regressed out for all variables)

	svPPA	Control	svPPA	svPPA vs Control	AD	AD	svPPA vs AD	AD vs Control
Left	**Mean±SD**	**Mean±SD**	**% of Control**	**p-value**	**Mean±SD**	**% of Control**	**p-value**	**p-value**
N	***12***	***23***			***36***			
Left ant H	832±99	1325±192	62.8	**<0.001**	1101±260	83.1	**0.002**	**0.002**
Left post H	1071±153	1356±101	79.0	**<0.001**	1080±196	79.7	0.484	**<0.001**
Left Ant/Post ratio	43.4±4.2	49.2±4.4	-	**0.001**	50.4±5.5		**<0.001**	0.603
N	***14***	***23***			***37***			
Right ant H	1242±253	1484±247	83.7	0.006	1196±234	80.6	0.535	**<0.001**
Right post H	1138±213	1276±172	89.2	0.039	1070±204	83.8	0.341	**<0.001**
Right Ant/Post ratio	51.9±6.1	53.5±6.8	-	0.360	53.2±5.4		0.452	0.893

*Bolded p-values are significant after the Holm-Bonferroni correction. Ant=anterior; post=posterior; H=hippocampus; svPPA=semantic variant Primary Progressive Aphasia; AD=Alzheimer's disease.

Table 3a.

Comparison of svPPA with healthy controls and AD on anterior and posterior hippocampal atrophy rates (% volume loss/year)

	svPPA	Control	svPPA vs Control	AD	svPPA vs AD	AD vs Control
Left	**Mean±SD**	**Mean±SD**	**p-value**	**Mean±SD**	**p-value**	**p-value**
N	***6***	***9***		***12***		
Left ant H	−4.00±3.94	−0.35±1.15	0.050	−0.79±2.46	0.067	0.754
Left post H	−4.42±2.70	−0.46±1.80	0.018	−1.89±4.47	0.151	0.382
N	***6***	***9***		***12***		
Right ant H	−2.89±3.64	−0.04±1.21	0.113	−1.84±1.73	0.385	0.023
Right post H	−3.81±3.96	−0.96±1.57	0.113	−1.87±2.98	0.291	0.651

*Bolded p-values are significant after the Holm-Bonferroni correction. Ant=anterior; post=posterior; H=hippocampus; svPPA=semantic variant Primary Progressive Aphasia; AD=Alzheimer's disease.

Table 4.

Comparison of svPPA with healthy controls and AD on MTL subregional volumes (in mm^3; parahippocampal subregions are corrected for slice number; ICV is regressed out for all variables)

	svPPA	Control	svPPA	svPPA vs Control	AD	AD	svPPA vs AD	AD vs Control
Left	**Mean±SD**	**Mean±SD**	**% of Control**	**p-value**	**Mean±SD**	**% of Control**	**p-value**	**p-value**
N	***12***	***23***			***36***			
CA1	831±129	1328±126	−37.4	**<0.001**	1043±219	−21.5	**0.002**	**<0.001**
DG	612±72	826±107	−25.9	**<0.001**	664±119	−19.7	0.068	**<0.001**
SUB	370±44	436±44	−15.2	**<0.001**	390±69	−10.7	0.220	0.012
ERC	15.7±3.4	21.1±2.5	−25.9	**<0.001**	18.8±4.2	−11.3	0.032	0.012
BA35	9.8±3.9	21.2±4.0	−53.8	**<0.001**	16.3±4.8	−23.3	**<0.001**	**<0.001**
BA36	33.0±10.6	71.5±12.2	−53.8	**<0.001**	63.2±17.4	−11.6	**<0.001**	0.076
PHC	42.1±9.1	55.3±9.6	−23.9	**0.001**	45.4±9.4	−17.9	0.283	**0.001**
Right	***Mean±SD***	***Mean±SD***	***% of Control***	***p-value***	***Mean±SD***	***% of Control***	***p-value***	***p-value***
N	***14***	***23***			***37***			
CA1	1157±208	1399±138	−17.3	**<0.001**	1133±210	−19.0	0.626	**<0.001**
DG	747±126	851±94	−12.2	0.010	666±109	−21.7	0.049	**<0.001**
SUB	403±50	438±42	−8.1	0.033	393±72	−10.4	0.535	0.003
ERC	19.4±4.8	22.2±3.4	−12.6	0.062	19.6±3.8	−11.9	0.916	0.011
BA35	16.9±5.9	21.3±2.6	−20.6	**0.002**	17.6±4.5	−17.4	0.447	**0.001**
BA36	46.3±16.4	69.4±11.7	−33.2	**<0.001**	64.8±17.2	−6.6	**0.002**	0.194
PHC	56.5±12.9	62.2±9.7	−9.2	0.156	49.7±11.5	−20.2	0.083	**<0.001**

*Bolded p-values are significant after the Holm-Bonferroni correction. svPPA=semantic variant Primary Progressive Aphasa; AD=Alzheimer's disease; CA=cornu ammonis; DG=dentate gyrus; SUB=subiculum; ERC=entorhinal cortex; BA=Brodmann area; PHC=parahippocampal cortex

Table 5a.

Comparison of svPPA with healthy controls and AD on MTL subregional atrophy rates (%/year)

	svPPA	Control	svPPA vs Control	AD	svPPA vs AD	AD vs Control
Left	**Mean±SD**	**Mean±SD**	**p-value**	**Mean±SD**	**p-value**	**p-value**
N	***6***	***9***		***12***		
CA1	−5.21±4.48	−0.98±1.98	0.066	−0.65±3.46	0.053	1.000
DG	−3.52±2.42	0.39±1.98	0.012	−1.25±4.26	0.102	0.422
SUB	−6.72±4.80	−1.21±2.06	0.036	−2.26±3.25	0.067	0.422
ERC	−3.92±4.55	−0.54±2.17	0.181	−3.34±2.79	0.964	0.015
BA35	−2.11±7.44	−1.53±2.36	0.689	−4.06±6.62	0.682	0.277
BA36	−8.57±5.63	−0.36±1.46	**<0.001**	−3.90±3.40	0.041	0.004
PHC	−5.01±3.92	0.42±2.06	0.012	−3.03±3.13	0.151	0.009
Right	***Mean±SD***	***Mean±SD***	***p-value***	***Mean±SD***	***p-value***	***p-value***
N	***6***	***9***		***12***		
CA1	−2.08±4.61	−0.04±1.17	0.113	−1.56±3.13	0.616	0.219
DG	−3.14±4.29	0.07±2.50	0.181	−0.59±7.27	0.616	0.277
SUB	−4.33±3.58	−1.05±2.47	0.113	−2.45±3.10	0.437	0.219
ERC	−2.17±3.87	−0.03±2.41	0.181	−4.02±3.82	0.437	0.023
BA35	−8.52±5.74	0.46±1.61	0.008	−6.05±3.78	0.385	**<0.001**
BA36	−9.02±3.22	0.12±1.79	**<0.001**	−3.86±2.62	0.003	**0.001**
PHC	−3.89±4.39	−0.36±1.71	0.145	−3.29±3.10	1.000	0.049

*Bolded p-values are significant after the Holm-Bonferroni correction. svPPA=semantic variant Primary Progressive Aphasia; AD=Alzheimer's disease; CA=cornu ammonis; DG=dentate gyrus; SUB=subiculum; ERC=entorhinal cortex; BA=Brodmann area; PHC=parahippocampal cortex